



## PH-24

### Effects of the “Source/ surface” and “Surface/sensor” Coupling and Colorimetric of Laser Speckle Pattern on the Performance of Optical Imaging System

Mohamed Darwish<sup>1</sup>, Ashraf F. El-Sherif<sup>2</sup>, Hatem El-Ghandour<sup>3</sup>, and Hussein A. Aly

#### Abstract

Optical imaging systems are widely used in different applications include tracking for portable scanners; input pointing devices for laptop computers, cell phones, and cameras, fingerprint-identification scanners, optical navigation for target tracking, and in optical computer mouse.

We presented an experimental work to measure and analyze the laser speckle pattern (LSP) produced from different optical sources (i.e. various color LEDs, 3 mW diode laser, and 10mW He-Ne laser) with different produced operating surfaces (Gabor hologram diffusers), and how they affects the performance of the optical imaging systems; speckle size and signal-to-noise ratio (*signal* is represented by the patches of the speckles that contain or carry information, and *noise* is represented by the whole remaining part of the selected image). The theoretical and experimental studies of the colorimetry (color correction is done in the color images captured by the optical imaging system to produce realistic color images which contains most of the information in the image by calculating the RGB components) for the used optical sources are investigated and introduced to present the relations between the signal-to-noise ratios with different diffusers for each light source.

From the experimental results, we found that the speckle size ranged from 4.59 to 4.62  $\mu\text{m}$ , which are slightly different or approximately the same for all produced diffusers. But, the calculated value of signal-to-noise ratio takes different values ranged from 0.69 to 0.92 for different diffuser, which means that surface texture will affects the performance of optical sensor based on laser speckle pattern used for optical imaging system.

<sup>1,2</sup> Engineering Physics Department, Military technical College, Cairo, Egypt.

<sup>3</sup> Physics Department, Faculty of Sciences, Ain Shams University, Cairo, Egypt.

<sup>4</sup> Computer Department, Military Technical College, Cairo, Egypt.

## 1. Introduction:

A laser speckle pattern (LSP) technique for designing an optical imaging system is presented. The LSP is used to determine the velocity of the device in a way that allows working on a wide class of surfaces and the operational principles of the laser speckle pattern technique are explained [1-10].

There are many parameters affecting the performance of optical imaging systems these parameters can be summarized in two main parameters which are:

- a) *The optical source*: which is responsible on selecting; the technique of operation, the operating surface, and the sensor type, and
- (b) *The optical sensor*: whose characteristics are highly dependent on the environmental conditions, like: *the surface nature, the source/surface coupling, the sensor/surface coupling, the working distance, and the speed of movement.*

*The objectives of this paper are:*

- i) Study and analyze the laser speckles produced from different optical sources and how it affects the performance of the optical imaging systems.
- ii) Study and analyze the laser speckles produced from different operating surfaces and how it affects the performance of the optical imaging systems.
- iii) Study the *source/surface* coupling and the *sensor/surface* coupling for the optical imaging systems based on a laser speckle technique.

In this paper we will introduce and explain each of these types of coupling and how it affects the performance of optical imaging systems, taking into consideration that the operating surface (diffuser), and light source are varied through the study, while the distances between optical elements, and sensor are maintained unchanged through the study.

## 2. Background on Colorimetry:

*Color* is the way the *human visual system* HVS interprets a part of the electromagnetic spectrum, approximately between 300 and 830 nm. Because of certain properties of the HVS we are not able to see all of the possible combinations of the visible spectrum but we tend to group various spectra into colors [11].

*Colorimetry* is the science and technology used to quantify and describe physically the human color perception, colorimetry has been extensively used in various color industries. Nowadays it is been increasingly used in the field of image processing due to the extensive development of cheaper and more advanced computer-controlled color displays, printing and scanning devices. Colorimetry applications can be divided into three areas: color specification, color difference and color appearance [12].

*Color image processing* is a developing field in science and technology. Applications include agriculture quality control, surveillance of vehicles or crowds, graphic arts, medical imaging case studies and industrial handling. In many cases images captured by the camera do not give a good quality color images, that is, variation in colour and brightness of an image due to artifacts, change in luminance and focus levels. Often color correction is necessary to get good quality images and many software packages are available to correct brightness, contrast, color and sharpness levels. However these softwares do not produce the color according to the perception of the HVS.

### 2.1 The CIE System:

The basis for colorimetry was established by CIE (Commission Internationale de l'Éclairage) in 1931 based on visual experiments. Even though they have some limitations, the CIE system

of colorimetry remains the only internationally agreed system for color measurements. All the color-related international standards and specifications use the CIE system. The CIE system provided a standard method for perceiving a color stimulus under controlled illuminating and viewing conditions. There are three key elements given by CIE system for color perception: spectral power distribution (light), reflectance spectrum (object), and color matching functions (which defines how human eyes match color stimuli using a set of red, green and blue reference primaries) [13].

## 2.2 Color Spaces:

A color space is a notation by which we can specify colors, i.e the human perception of the visible electromagnetic spectrum. Color space is described as an abstract mathematical model, in which colors are represented numerically. The main aim of the development of the color spaces was to provide uniform performance for the measurement of color differences. Different color spaces are better for different applications, and many factors are considered for using different color spaces. There are some terms we need for describing color spaces which are [11]:

- *Brightness*: This is the human sensation by which an area exhibits more or less light.
- *Lightness*: This is the sensation of an area's brightness relative to a reference white in the scene.
- *Hue*: The human sensation according to which an area appears to be similar to one, or proportions of two, of the perceived opposing colors red, yellow, green and blue.
- *Colorfulness*: The human sensation according to which an area appears to exhibit more or less of its hue.
- *Chroma*: The colorfulness of an area relative to the brightness of a reference white.
- *Saturation*: The colorfulness of an area relative to its brightness.

## 2.3 Classification of Color Spaces:

Color spaces can be classified into three main categories which are [14, 15]:

- HVS based color spaces, which include the RGB color space, the opponent colors theory based color spaces and the phenomenal color spaces. These color spaces are motivated by the properties of the HVS.
- Application specific color spaces, which include the color spaces adopted from TV systems (YUV, YIQ), photo systems (Kodak Photo YCC) and printing systems (CMY(K))
- CIE color spaces, which are spaces proposed by the CIE and have some properties of high importance like device-independency and perceptual linearity (CIE XYZ, Lab and Luv)

## 2.4 XYZ Color Space:

XYZ color space is basically a three valued system that models the appearance of color by human eye. This method, established and developed by the Commission Internationale de l'Éclairage (CIE) [16], needs to include the specifications of the observer, light source, device, and other aspects of the viewing conditions.

The CIE XYZ color space defines all the colors in terms of three imaginary primaries X, Y, and Z based on the human visual system. The X, Y, Z tristimulus values of a color stimulus ( $S(\lambda)$ ) which represent the luminance or lightness of the colors are expressed as:

$$\begin{aligned}
X &= K \int_{380nm}^{780nm} S(\lambda) \bar{x}(\lambda) d\lambda \\
Y &= K \int_{380nm}^{780nm} S(\lambda) \bar{y}(\lambda) d\lambda \\
Z &= K \int_{380nm}^{780nm} S(\lambda) \bar{z}(\lambda) d\lambda
\end{aligned}
\tag{1}$$

Where,  $\bar{x}(\lambda)$ ,  $\bar{y}(\lambda)$  and  $\bar{z}(\lambda)$  are the color matching functions,  $S(\lambda)$  represents the spectral radiometric quantity at a certain wavelength  $\lambda$ , e.g., it is the light transmission intensity in a practical device, and  $k$  is a proportionality constant that relates spectral radiance [17] or spectral radiant power [18], with spectral irradiance  $S(\lambda)$  [19, 20].

Equation (1) can be expressed in terms of the unitary spectral irradiance  $U(\lambda)=S(\lambda)/S_{peak}$ , where  $S_{peak} = S(\lambda_{peak})$ , to provide tristimulus expressions that linearly depend on peak irradiance:

$$\begin{aligned}
X &= KE_{peak} \int_{380nm}^{780nm} U(\lambda) \bar{x}(\lambda) d\lambda = KS_{peak} \hat{X} \\
y &= KE_{peak} \int_{380nm}^{780nm} U(\lambda) \bar{y}(\lambda) d\lambda = KS_{peak} \hat{Y} \\
z &= KE_{peak} \int_{380nm}^{780nm} U(\lambda) \bar{z}(\lambda) d\lambda = KS_{peak} \hat{Z}
\end{aligned}
\tag{2}$$

Where  $\hat{X}$ ,  $\hat{Y}$  and  $\hat{Z}$  are the normalized tristimulus values, which for practical purposes remain almost constant when the emitted power changes. This approximation is valid for LEDs because peak wavelength and spectral width do not change considerably when adjusting the drive current [21, 22].

A simple yet sufficiently accurate mathematical model for the relative spectrum  $U(\lambda)$  of an LED is given by [23]:

$$U(\lambda) = \frac{1}{3} [g(\lambda) + 2g^5(\lambda)]
\tag{3}$$

Where  $g(\lambda)=\exp\{-[(\lambda -\lambda_i)/ \Delta\lambda_i]^2\}$ ,  $\lambda_i$  is the peak wavelength and  $\Delta\lambda_i$  is the half spectral width.

## 2.5 RGB Color Space:

This color space is considered as a basic one because of its wide use in color cameras, scanners, projectors and displays with direct RGB signal input or output [24]. The main idea that led to the specification of the RGB color space was; if we manage to describe the visible spectrum in such a way that simulates the very first detection of light in the human eye, we have all the information needed for the storage, processing and generation (visualization) of a perceptually equivalent spectrum. This idea implies certain knowledge of the acquirement of visual information by the human visual system. The trichromatic theory (based on the work of Maxwell, Young and Helmholtz) states that there are three types of photoreceptors, approximately sensitive to the red, green and blue region of the spectrum.

Each color in this space is described by three components R, G and B. The value of these components is the sum of the respective sensitivity functions and the incoming light which is given by:

$$R = K \int_{380}^{780} S(\lambda) R(\lambda) d\lambda$$

$$G = K \int_{380}^{780} S(\lambda)G(\lambda)d\lambda \quad (4)$$

$$B = K \int_{380}^{780} S(\lambda)B(\lambda)d\lambda$$

Where  $S(\lambda)$  is the light spectrum,  $R(\lambda)$ ,  $G(\lambda)$  and  $B(\lambda)$  are the sensitivity functions for the  $R$ ,  $G$  and  $B$  sensors, respectively.

As we can see from the above equations, the RGB values depend on the specific sensitivity function of the capturing device. This makes the RGB color space a device-dependant color space. Printing and displaying devices also works on an RGB-fashion basis. And they also have their specific sensitivity functions which makes the term *controlled environment* even more difficult to achieve.

## 2.6 Color Space Conversions:

Color space conversion is used to change one type of color signal present in the image to other. It mainly depends on the input and output device used and also the format of the image. In some cases to find the values of the RGB, CIE XYZ color space is used and then converted back to RGB. XYZ to RGB conversion can be done using this matrix transform [25].

$$\begin{bmatrix} R \\ G \\ B \end{bmatrix} = \begin{bmatrix} 3.2405 & -1.5371 & -0.4985 \\ -0.9693 & 1.8760 & 0.0416 \\ 0.0556 & -0.2040 & 1.0572 \end{bmatrix} \begin{bmatrix} X \\ Y \\ Z \end{bmatrix} \quad (5)$$

## 3. Experimental Work:

### 3.1 Light Sources Spectrum Measurements:

Since the performance of the optical imaging system is highly dependent on the used light source so, it is very important to study and measure the spectrum of the used sources. The measurement of the spectrum is performed by means of the experimental arrangement which is shown schematically in Figure (1) and the photograph of this arrangement is reproduced in Figure (2).

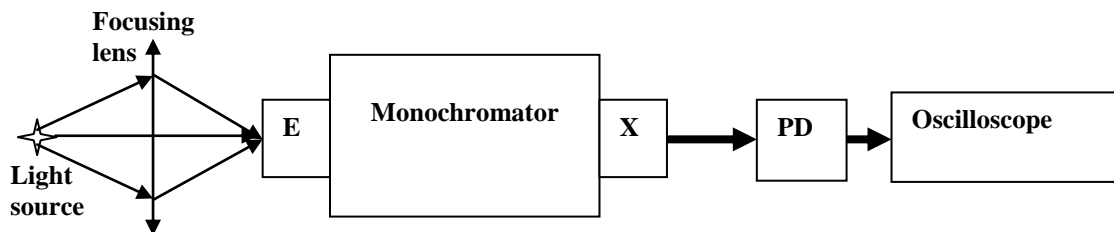
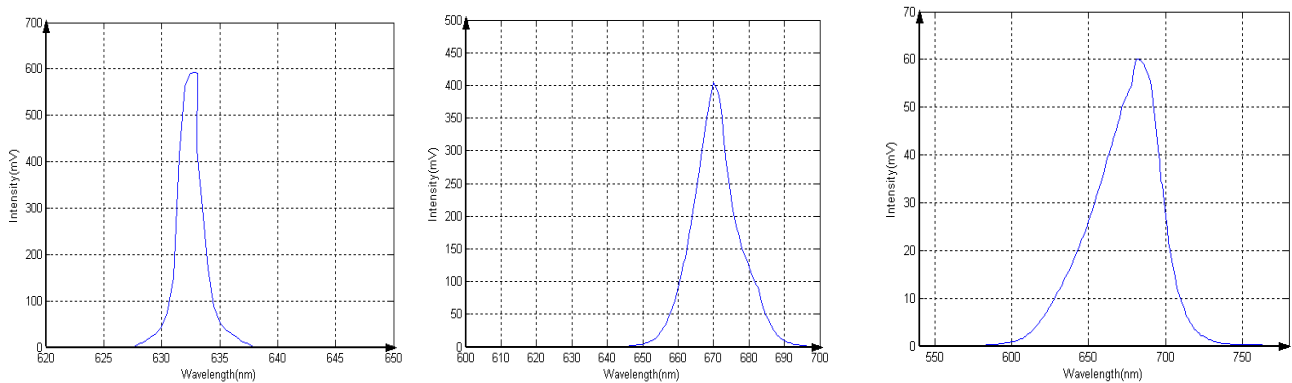


Fig.1. A schematic diagram to measure the spectrum of light sources.

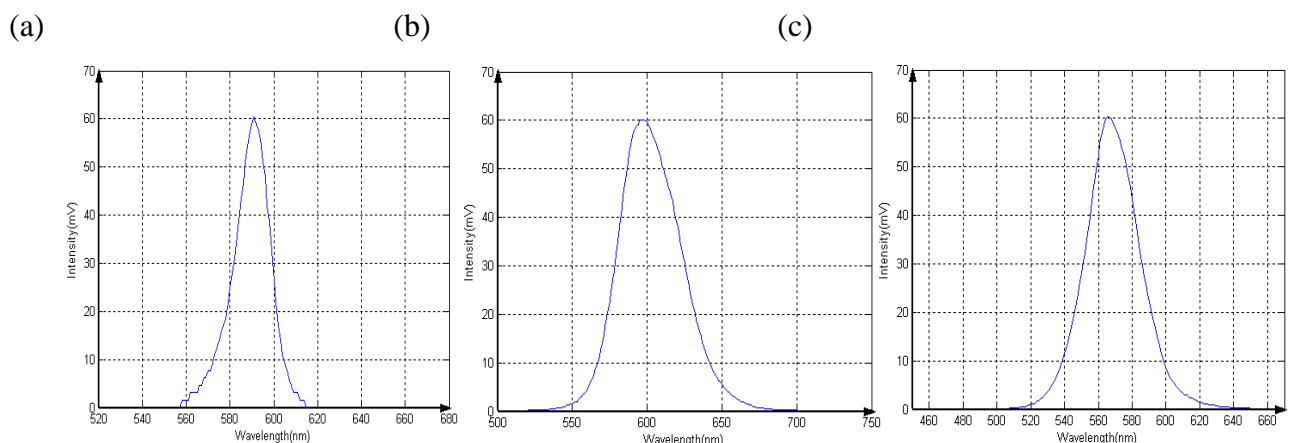


Fig.2. Experimental set-up to measure the spectrum of light sources.

As shown in this figure the arrangement consists of a light source (which is required to be measured), focusing lens, monochromator (CHROMEX, Model 500SM), silicon



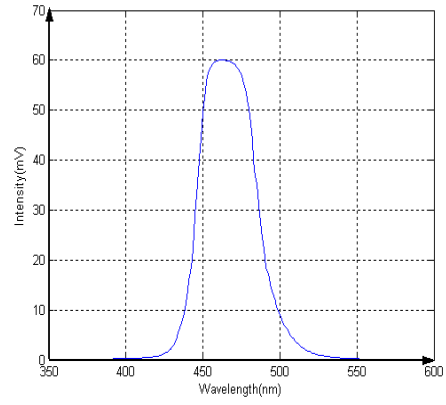
photodetector (PHYWE, Model 08735), and oscilloscope (TEKTRONIX, Model TDS 220). The incident light beams, either from laser source [He-Ne laser (Spectra-Physics INC., Model 105-1,  $\lambda=632.8\text{nm}$ ,  $P=10\text{mw}$ ) or diode laser (RS, Model 194-032,  $\lambda=670\text{nm}$ ,  $P=2.8\text{mw}$ )] or from LED source (different commercial colored LEDs) are collimated by the focusing lens to fall on the monochromator's entrance slit E and the output from the monochromator's exit slit X is allowed to fall on the photodetector PD whose output is introduced to oscilloscope (as a voltage levels corresponding to the light intensity) which is interfaced to a computer through a WAVESTAR SOFTWARE to be stored. The spectrum is measured by adjusting the monochromator to scan from wavelength 380nm to 780nm by step 1nm and scan rate 1nm/sec and the interface software is adjusted to store one reading per second. The stored data is then drawn using Matlab program. The measured spectrum curves are shown in the Figure (3) and the measured data is shown in table 1:



(d)

(e)

(f)



(g)

Fig. 3 The spectrum of (a) He-Ne laser (b) diode laser (c) red LED (d) orange LED (e) yellow LED (f) green LED (g) blue LED

Table-1 The measured spectrum of light sources:

Source	Band of spectrum	Central peak	Band width
He-Ne laser	From 629nm to 636.5nm	At 632.8nm	1.5nm
Diode laser	From 646nm to 696nm	At 670nm	7nm
Red led	From 582nm to 769nm	At 682nm	30nm
Orange led	From 512nm to 703nm	At 597nm	35nm
Yellow led	From 557nm to 614nm	At 591nm	12nm
Green led	From 502nm to 659nm	At 566nm	24nm
Blue led	From 392nm to 571nm	At 463nm	34nm

### 3.2 Production of Speckle Pattern:

Different diffusers [26, 27] are used as rough objects for production of speckle patterns. These patterns are recorded photographically making use of the set-up shown in Figure (4) and the photograph of this arrangement is reproduced in Figure (5).

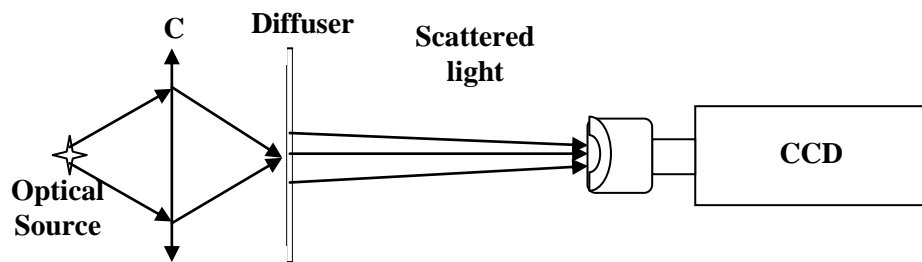


Fig. 4. Schematic diagram for the arrangement of recording speckle pattern



Fig. 5. Experimental set-up for recording speckle pattern

In the experimental set-up, a light beam from different types of light sources [He-Ne laser, Diode laser and (Red, Blue, Green, Yellow and Orange LEDs)] is used to illuminate different surfaces (glass diffusers) through a focusing lens  $C_1$ . The scattered light is recorded using a high performance color coupled charge device (CCD camera, Model 8313-1000, COHU Company) which is placed in front of the diffuser. The obtained speckle images recorded using the different diffusers with the mentioned sources after making some enhancement are shown in Figures (6-10).



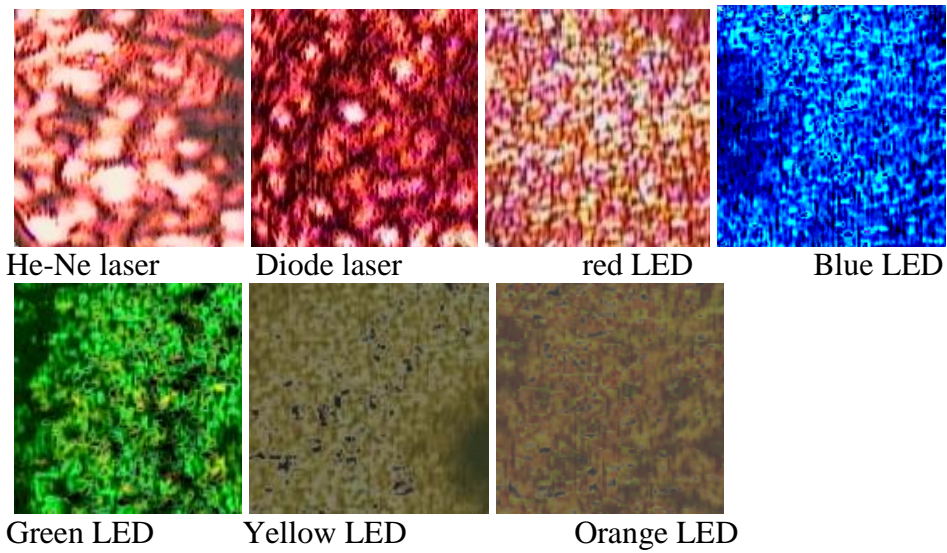


Fig. 6 The speckle images produced from a diffuser whose  $L=0.014\text{cm}$  with different light sources.

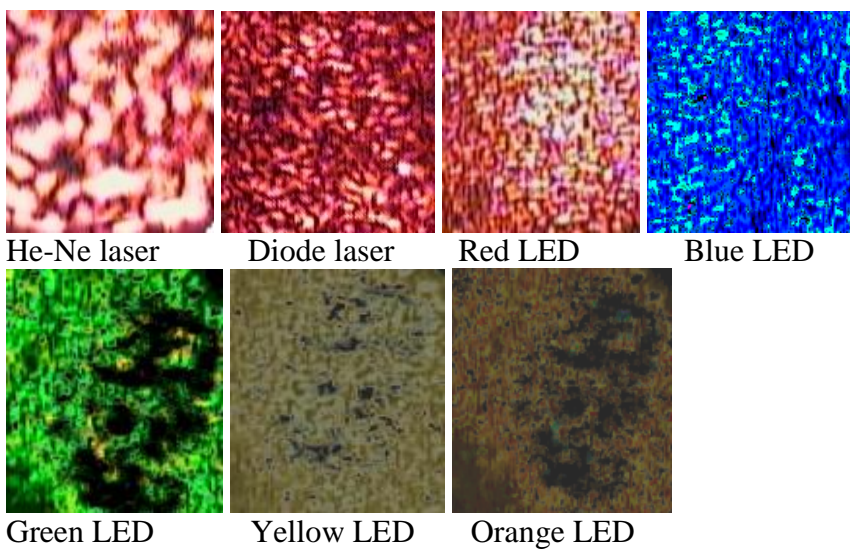
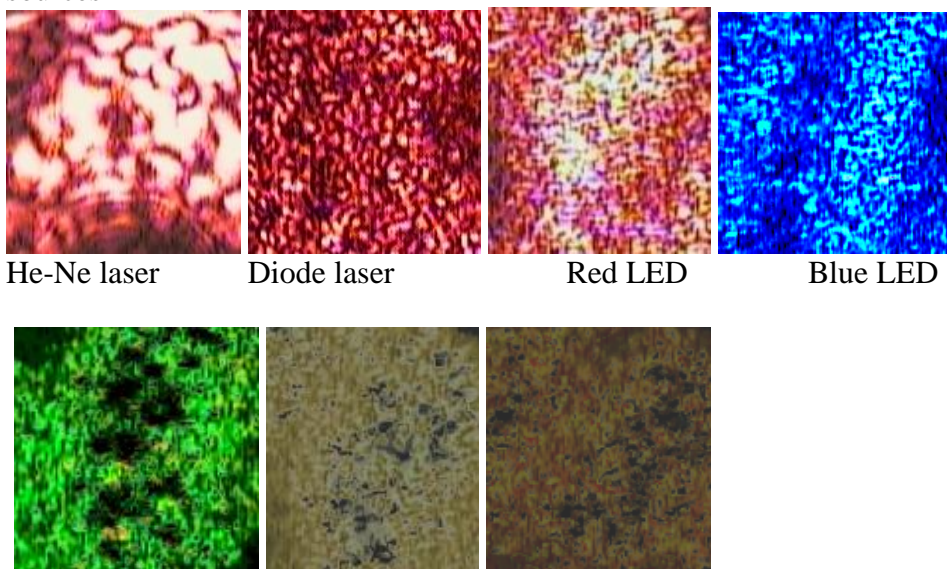
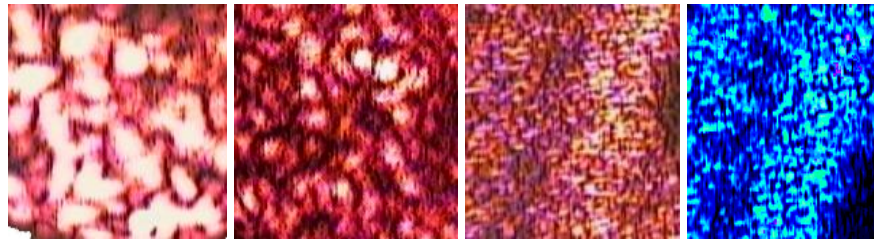


Fig.7 The speckle images produced from a diffuser whose  $L=0.056\text{cm}$  with different light sources

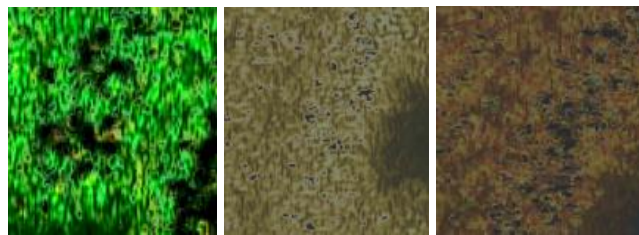


Green LED      Yellow LED      Orange LED

Fig.8 The speckle images produced from a diffuser whose  $L=0.08\text{cm}$  with different light sources

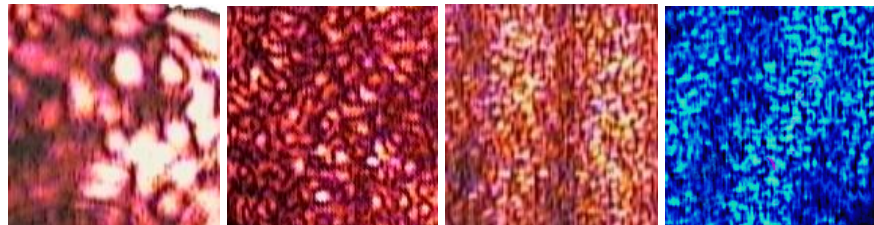


He-Ne laser      Diode laser      Red LED      Blue LED

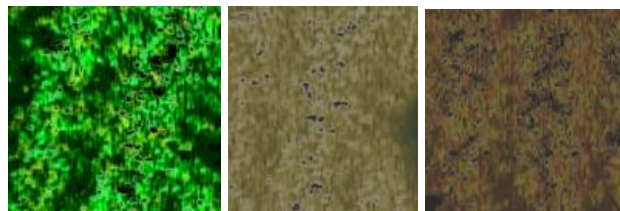


Green LED      Yellow LED      Orange LED

Fig.9 The speckle images produced from a diffuser whose  $L=0.093\text{cm}$  with different light sources



He-Ne laser      Diode laser      Red LED      Blue LED



Green LED      Yellow LED      Orange LED

Fig.10 The speckle images produced from a diffuser whose  $L=0.13\text{cm}$  with different light sources.

#### 4. Results and Discussion:

##### 4.1 RGB components calculation:

For accurate analysis to the speckle images, MatLab program is introduced to select suitable gray scale which contains most of the informative data in the image, this is done by calculating the accurate Red-Green-Blue (RGB) color components making use of the measured spectrum for light sources introduced previously, and color matching functions  $\bar{x}(\lambda)$ ,  $\bar{y}(\lambda)$  and  $\bar{z}(\lambda)$  of International Telecommunication Organization (ITU-R709) for CRT



phosphorus, Tirinton-SONY Model. The resultant RGB values for all sources are shown in table 2.

Table- 2 The RGB values of the used sources:

Source	Red value (R)	Green value (G)	Blue value (B)
He-Ne laser	0.8681	0.1041	0.0278
Diode laser	0.7486	0.1938	0.0576
Red LED	0.9664	0	0
Orange LED	1	0.3240	0
Yellow LED	1	0.4675	0
Green LED	0	0.85	0
Blue LED	0	0.131233	0.86877

#### 4.2 Speckle Image Analysis:

Computer image processing program using MatLab software has been introduced to analyze the speckle images. In MatLab program, the colored image is converted into gray image using the calculated RGB components (mentioned in table.2), then by selecting a suitable intensity threshold level we convert this digital gray image (0 - 255) to a binary image. A binary [0, 1] image is obtained, where zero is taken to represent the background while one is used to represent the spatial information of speckle grains, where the intensity below 50% is considered as background. Knowing that the software program operates in a circular region of the image (with diameter equal to the spot diameter) whose size is equal to 249600 pixels to obtain accurate calculations. Figures (11-15) show the operation of the Matlab program in the speckle images produced using He-Ne laser. Each figure includes the colored image, the digital random gray scale image, the digital accurate RGB gray image, the binary random gray scale image, and the binary accurate RGB gray image. From these figures we can observe how most information lost in the case of using random gray scale.

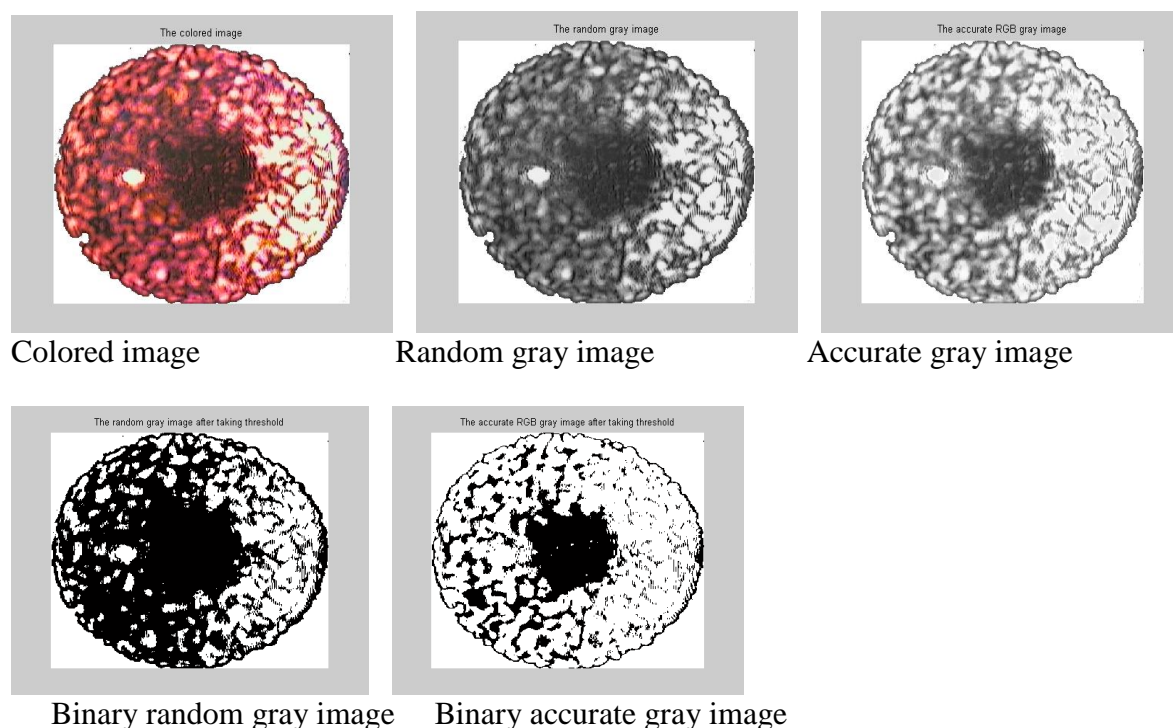
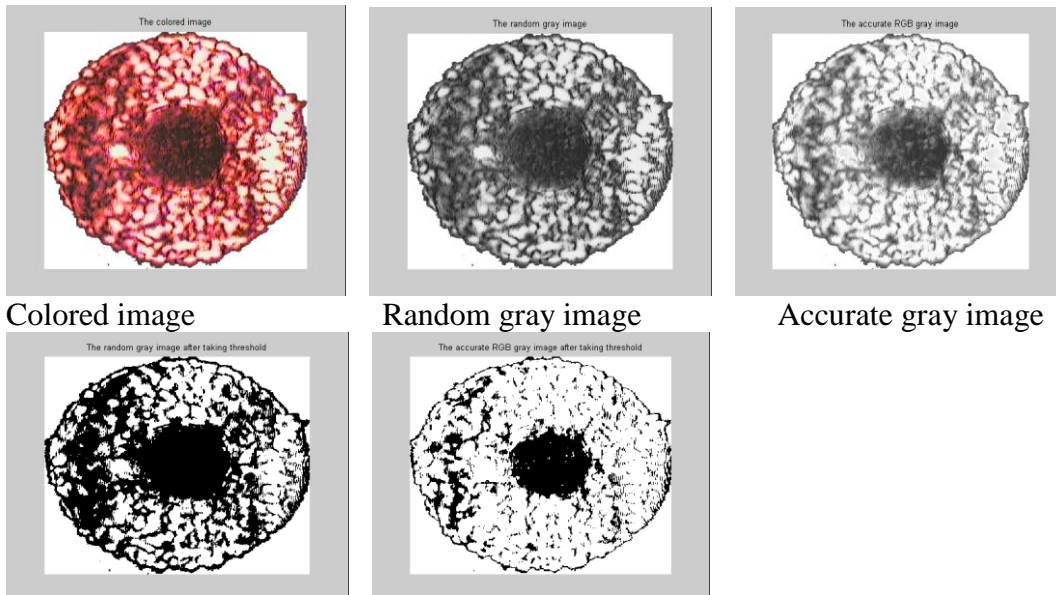
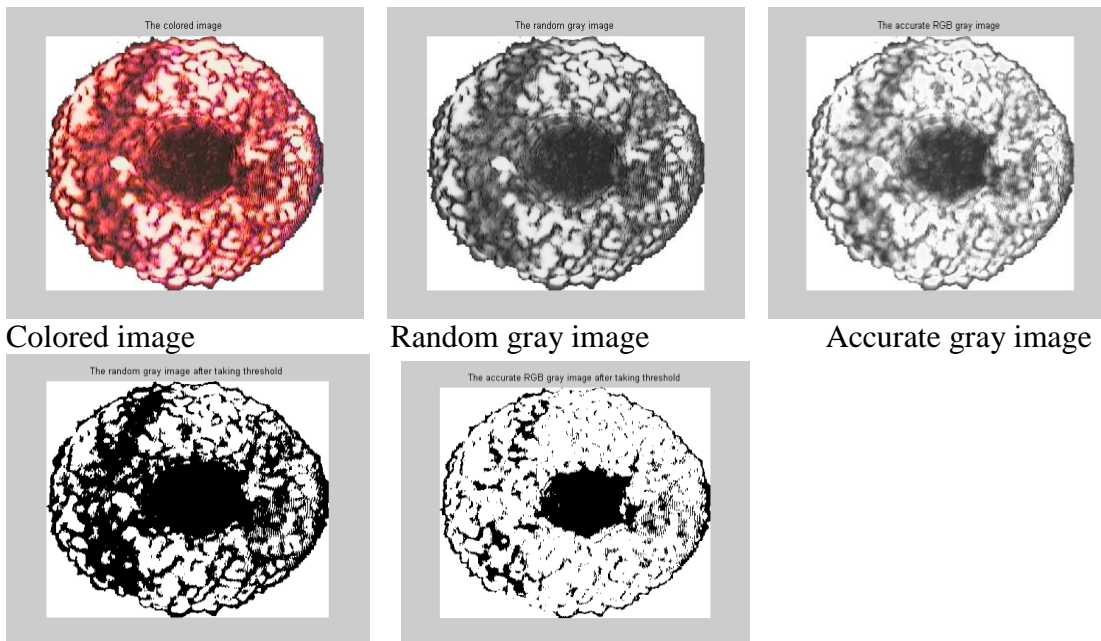


Fig.11 Image processing done on speckle images produced using He-Ne laser with the diffuser (L=0.014cm)



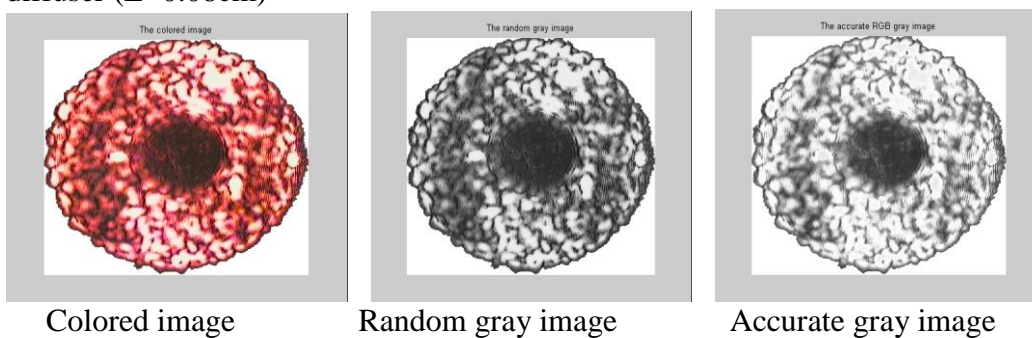
Binary random gray image    Binary accurate gray image

Fig.12 Image processing done on speckle images produced using He-Ne laser with the diffuser ( $L=0.056\text{cm}$ )



Binary random gray image    Binary accurate gray image

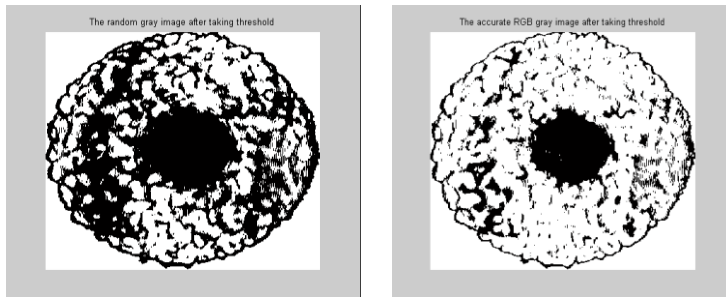
Fig.13 Image processing done on speckle images produced using He-Ne laser with the diffuser ( $L=0.08\text{cm}$ )



Colored image

Random gray image

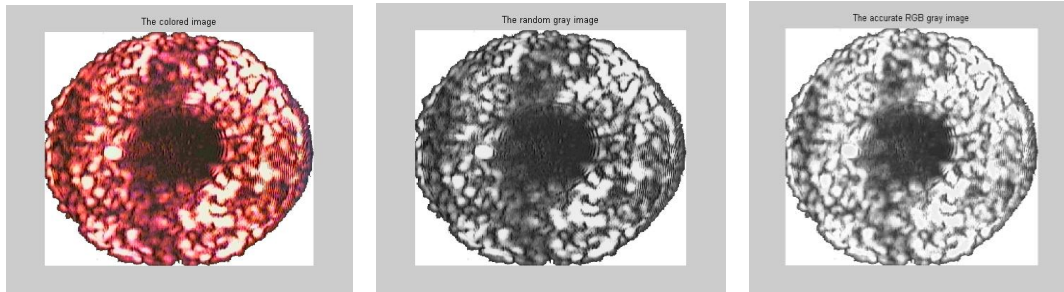
Accurate gray image



Binary random gray image

Binary accurate gray image

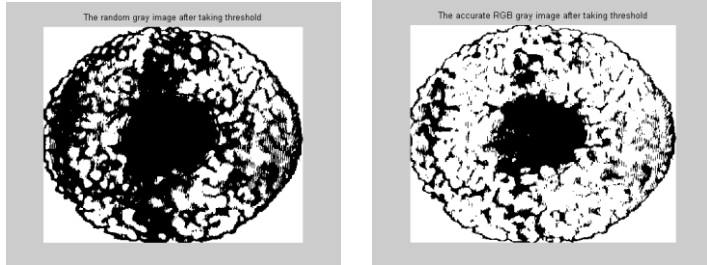
Fig.14 Image processing done on speckle images produced using He-Ne laser with the diffuser (L=0.093cm)



Colored image

Random gray image

Accurate gray image



Binary random gray image

Binary accurate gray image

Fig.15 Image processing done on speckle images produced using He-Ne laser with the diffuser (L=0.13cm)

By considering  $A_S$  to represent the patches of the speckle image that contains information and  $A_T$  to represent the whole part of the selected image, the ratio  $A_S/A_T$  is computed which gives a good indication about the resultant effective signal- to -noise ratio. From the obtained values of the ratio ( $A_S/A_T$ ), it is found that the signal- to-noise ratio varies for each speckle image. This variation is due to the random behavior of the speckle diffraction pattern obtained from a randomly distributed function of the rough surfaces with each light source. The calculated values of the ratio ( $A_S/A_T$ ) for the used five diffusers with the used seven light sources [26] are shown in table 3.

Table- 3 The values of signal-to-noise ratio ( $A_S/A_T$ ) for different diffusers with different light sources:

Diffuser $\lambda$ (nm)	L=0.014cm	L=0.056cm	L=0.08cm	L=0.093cm	L=0.13cm
633	0.769712	0.915335	0.891217	0.831669	0.716193
670	0.679306	0.724612	0.683167	0.639019	0.581588
697	0.398098	0.403626	0.438707	0.368288	0.353514
611	0.324787	0.307271	0.283587	0.312217	0.243116
567	0.148646	0.114181	0.150815	0.160285	0.086845
556	0.342275	0.406363	0.417833	0.379551	0.346152
460	0.357532	0.295007	0.361594	0.404336	0.430718

### 4.3 "Source/Surface" Coupling:

This type of coupling can be discussed by relating the values of signal-to-noise ratio ( $A_S/A_T$ ) and wavelength of used light sources (which is obtained in table 3) for each surface (diffuser). By source/surface coupling we denote that for each diffuser the setup of the system does not change (same distances between optical elements, same sensor [CCD camera], same surface) but with different light sources. The curves representing these relations for all used diffusers are shown in Figure (16).

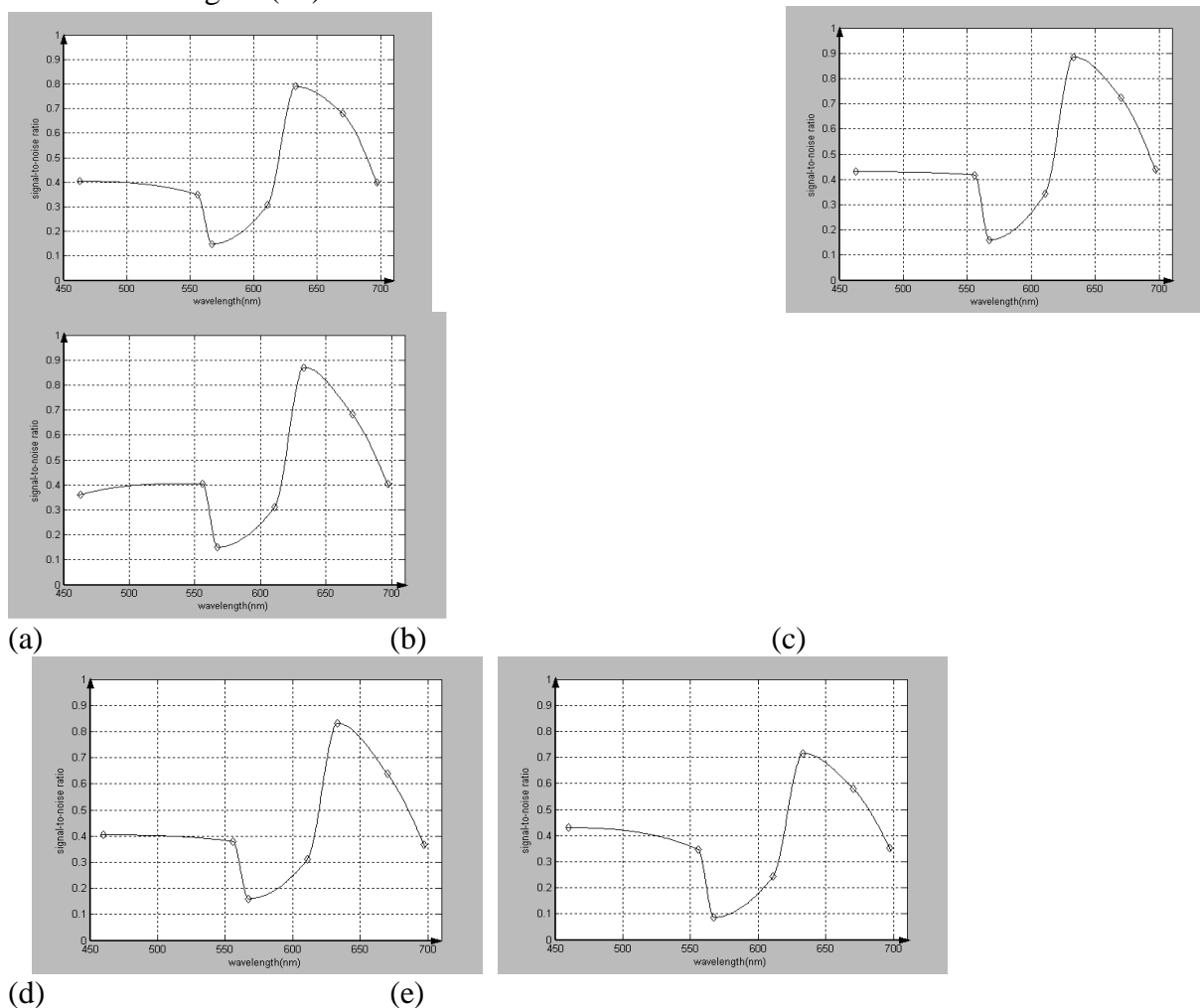


Fig.16 Relation between wavelength and signal-to-noise ratio for (a)  $L=0.014$  (b)  $L=0.056$  (c)  $L=0.08$  (d)  $L=0.093$  (e)  $L=0.13$

### 4.4 "Surface/Sensor" Coupling:

This type of coupling can be discussed by relating the values of signal-to-noise ratio ( $A_S/A_T$ ) and ( $L$ ) for each light source. By surface/sensor coupling we denote that for each light source the setup of the system does not change (same distances between optical elements, same sensor [CCD camera], same source) but with different surfaces (diffusers). The curves representing these relations for all used sources shown in fig.17 and from these curves we conclude that: For each light source the diffusers can be ordered from the best to the worst as shown in the table 4.

Table- 4 The values of signal-to-noise ratio ( $A_S/A_T$ ) for different diffusers with different light sources:

Light source	Best <span style="display: inline-block; width: 100px; border-bottom: 1px solid black;"></span> worst <span style="display: inline-block; width: 100px; border-bottom: 1px solid black;"></span> <span style="font-size: 2em;">→</span>				
	He-Ne laser	$L=0.056\text{cm}$	$L=0.08\text{cm}$	$L=0.093\text{cm}$	$L=0.014\text{cm}$

diode laser	L=0.056cm	L=0.08cm	L=0.014cm	L=0.093cm	L=0.13cm
red LED	L=0.08cm	L=0.056cm	L=0.014cm	L=0.093cm	L=0.13cm
orange LED	L=0.014cm	L=0.093cm	L=0.056cm	L=0.08cm	L=0.13cm
yellow LED	L=0.093cm	L=0.08cm	L=0.014cm	L=0.056cm	L=0.13cm
green LED	L=0.08cm	L=0.056cm	L=0.093cm	L=0.13cm	L=0.014cm
blue LED	L=0.13cm	L=0.093cm	L=0.08cm	L=0.014cm	L=0.056cm

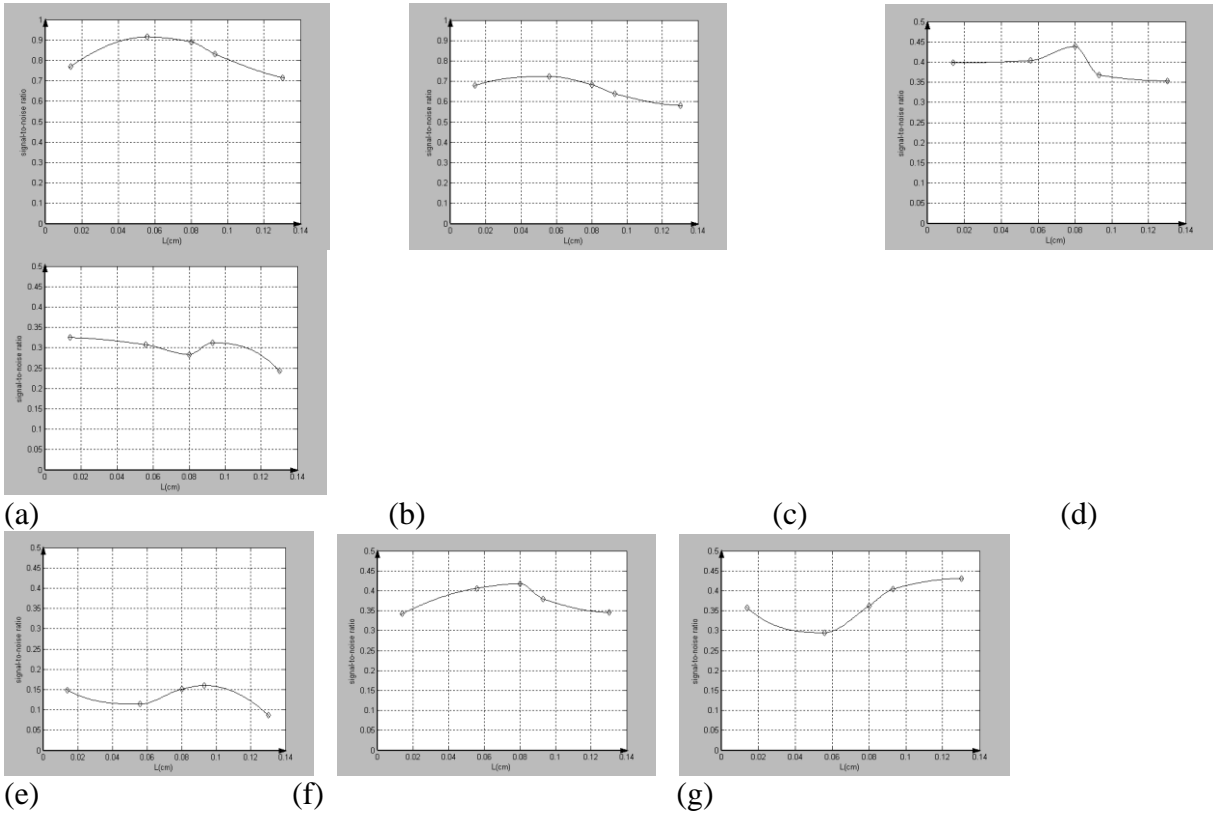


Fig.17 Relation between L and signal-to-noise ratio for (a)He-Ne laser (b) diode laser (c) red LED (d) orange LED (e) yellow LED (f) green LED (g) blue LED

#### 4.5 Case Study:

Let us consider the case of He-Ne laser, the speckle size is calculated using (Adobe Photoshop Program) by measuring the size of each bright in the speckle image both in the x and y directions and taking the average of the all measured values. The measurement is done accurately by dividing the measured value on a scale factor obtained from the scale image (this image is taken by removing the glass diffuser from the optical set-up shown in Figure (4) and placing a transparent scale in its position and illuminating the scale by the source to capture an image to the scale using CCD camera). The measured values of the speckle size for all diffusers are summarized and shown in table (5).

Table- 5 Speckle size and signal-to-noise ratio obtained using He-Ne laser with different diffusers:

Diffuser	L= 0.014cm	L= 0.056cm	L= 0.08cm	L= 0.093cm	L= 0.13cm
Speckle size ( $\mu\text{m}$ )	4.62576	4.61089	4.62123	4.62757	4.59801
Signal-to-noise ratio	0.7697122	0.9153352	0.8912169	0.8316686	0.7161931

Theoretically:

The speckle size can be calculated theoretically as follows:

$$\frac{\lambda d}{a}$$

The speckle size ( $\delta$ ) =  $a$

(6) Where:  $\lambda$  is the wavelength of the light source (632.8nm),  $d$  is the distance between the source and the surface (18.5cm), and  $a$  is the diameter of the laser spotlight (2.5cm), Then:

$$\delta = \frac{(632.8 * 10^{-6}) * (0.185)}{0.025} = 4.68272 * 10^{-6} m$$

From the measured values we found that the speckle size is almost the same for all diffusers (which satisfies the fact that the speckle size is independent on the illuminating surface) but, the value of signal-to-noise ratio takes different values for each diffuser. This means that the surface texture affects the performance of the optical sensor because, all images captured for all diffusers under the same conditions [same source (He-Ne laser), same distances of the experimental set-up, and the same sensor (CCD camera)].

### 5. Conclusions and Discussions:

The speckle images produced from different light sources with different surfaces were captured and analyzed using image processing program based on the RGB values and the values of signal-to-noise ratio was calculated for each case.

The source surface coupling has been discussed and concludes that:

- For all diffusers the maximum signal-to-noise ratio was obtained for the case of laser sources (He-Ne laser, and then diode laser).
- For all diffusers the minimum signal- to -noise ratio was obtained in the case of yellow LED, and then orange LED.
- For the case of red, green, and blue LEDs we can see that:
  1. For diffuser whose (L=0.014cm) the signal- to -noise ratio was high for red LED, moderate for blue LED, and low for green LED.
  2. For diffuser whose (L=0.056cm) the signal- to -noise ratio was high for green LED, moderate for red LED, and low for blue LED.
  3. For diffuser whose (L=0.08cm) the signal- to -noise ratio was high for red LED, moderate for green LED, and low for blue LED.
  4. For diffuser whose (L=0.093cm) the signal- to -noise ratio was high for blue LED, moderate for green LED, and low for red LED.
  5. For diffuser whose (L=0.13cm) the signal- to -noise ratio was high for blue LED, moderate for red LED, and low for green LED.

The sensor/surface coupling has been discussed and concludes that the performance of the optical imaging system for certain source varies from worst to best based on the operating surface as presented in table (4).

For the case study of the sensor /surface coupling for He-Ne laser the speckle size is almost the same for all diffusers (which satisfies the fact that the speckle size is independent on the illuminating surface) but, the value of signal-to-noise ratio takes different values for each diffuser. This means that the surface texture affects the performance of the optical sensor because, all images captured for all diffusers under the same conditions [same source (He-Ne laser), same distances of the experimental set-up, and the same sensor (CCD camera)].



## References:

- [1] Gary Gordon, John Corcoran, Jason Hartlove, Travis Blalock, Agilent Technologies, “Silicon Optical Navigation”, United States Patent No. 7643007, (Jan. 2010), with US Patent References: "[Method of operating an optical mouse](#)", October, (2005) – No. 20050231483, and "[Optical mouse with uniform level detection method](#)", October, (2005) – No. 20050231484.
- [2] F. Santos, V. Silva, L. Almeida, “A Robust Self-localization system for a Small Mobile Autonomous Robot”, in Proceedings of the IEEE International Symposium on Robotics and Automation, Toluca, Mexico, September 1–4, 2002.
- [3] S.P.N. Singh, K.J. Waldron, “Design and evaluation of an integrated planar localization method for desktop robotics”, in Proceedings of the IEEE International Symposium on Robotics and Automation, New Orleans, April 26–May 1, 2004.
- [4] J. Cooney, W.L. Xu, G. Bright, “Visual dead-reckoning for motion control of a Mecanum-wheeled mobile robot”, *Mechatronics* 14, p.623–637, 2004.
- [5] T.W. Ng, “The optical mouse as a two-dimensional displacement sensor”, *Sens. Actuators A* 107, p. 21–25, 2003.
- [6] K.-M. Lee, D. Zhou, “A real time optical sensor for simultaneous measurement of three-DOF motions”, *IEEE/ASME Trans. Mech.* 9 p.499–507, 2004.
- [7] T.W. Ng, K.T. Ang, “The optical mouse for vibratory motion sensing”, *Sens. Actuators A* 116, p.205–208, 2004.
- [8] T.W. Ng, K.T. Ang, “The optical mouse for harmonic oscillator experimentation”, *Am. J. Phys.* 73, p. 793–795, 2005.
- [9] Umberto Minoni, Andrea Signorini, “Low-cost optical motion sensors: An experimental characterization”, Elsevier B.V., 402-408, 2006.
- [10] P. Popov, S. Pulov, V. Pulov, “A laser speckle pattern technique for designing an optical computer mouse”, *Optics and Lasers in Engineering* 42, p.21–26, 2004.
- [11] S. J. Sangwine and R. E. N. Horne “The Color Image Processing Handbook”, Chapman & Hall, 1998.
- [12] Hsien-Che Lee, “Introduction to Color Imaging Science”, Cambridge University press, 2005.
- [13] Yoshi Ohno., “CIE Fundamentals for Color Measurements”, International Conference on Digital Printing Technologies, ISBN/ISSN: 0-89208-230-5, p. 540-545, 2000.
- [14] Charles Poynton, Frequently Asked Questions about Color, "<http://www.inforamp.net/poynton>", 1999.
- [15] Gunter Wyszecki, W.S. Stiles, “Color Science Concepts and Methods, Quantitative Data and Formulae”, John Wiley and Sons, Inc, 2000.
- [16] G. Wyszecki and W. Stiles, “Color Science Concepts and Methods, Quantitative Data and Formulae”, (2<sup>nd</sup> Edition), Wiley, New York, 1982.
- [17] D. Malacara, “Color Vision and Colorimetry”, SPIE Press, Bellingham WA, USA, 2002.
- [18] Henryk Palus, “Colour Spaces”, Chapman and Hall, 1998.
- [19] Y. Ohno, “Radiometry and Photometry Review for Vision Optics”, in *Handbook of Optics* (Vol. III, 2<sup>nd</sup> ed.), M. Bass, J. M. Enoch, E. W. Van Stryland, W. L. Wolfe, Eds, McGraw-Hill, 2001.
- [20] M. Strojnik, G. Paez, “Radiometry”, in *Handbook of Optical Engineering*, D. Malacara, B. Thompson, Eds., 2001.
- [21] Y. Uchida, T. Taguchi, “Lighting theory and luminous characteristics of white light-emitting diodes”, *Opt. Eng.* 44, 124003–1, 2005.
- [22] Y. Gu, N. Narendran, T. Dong, H. Wu, “Spectral and luminous efficacy change of high-power LEDs under different dimming methods,” in *Sixth International Conference on Solid State Lighting*, I. T. Ferguson, N. Narendran, T. Taguchi, I. E. Ashdown, eds., Proc. SPIE 6337, 63370J:1-7, 2006.

- [23] Y. Ohno, "Spectral design considerations for white LED color rendering", *Opt. Eng.* 44, 111302-1 2005.
- [24] Charles Poynton, "A Guided Tour of Color Space, New Foundations for Video Technology", Proceedings of the SMTPE Advanced Television and Electronic Imaging Conference, p. 167-180, 1995.
- [25] Adrian Ford and Alan Roberts, "Color space conversions", Westminster University, London, 1998.
- [26] El Ghandoor, H., Ashraf F. El-Sherif, Darwish, M., "Designing a new optical sensor using wide band speckle patterns", in *Optical Measurement Systems for Industrial Inspection V*, Optical Metrology Conference 2007, Proceedings of SPIE Vol. 6616, Germany, 2007.
- [27] M. Darwish , Ashraf F. El-Sherif, and Hatem El Ghandoor, "Application of Gabor Hologram for Designing a New Optical Imaging System", *Mathematics and Engineering Physics Conference*, 4th International Conference of the MTC, Cairo, Egypt, 2008.